Enabling Perspective Multiplication for Multi-Perspective Enrollment with University of Twente Finger Vein Scanner

Koen Rikkerink[1]

Abstract

This research will focus on improving the current Finger Vein Scanner by enhancing Image quality and implementing Perspective Multiplication for Multi-Perspective Enrollment. In addition a new protocol is established: Full PM-MPE. This protocol will compare all images with their corresponding pseudo-perspectives to PM-MPE.

CONTENTS

*This work was supported by the Data Science Group

[1] K.B.W. Rikkerink is an Embedded Systems Master student at the University of Twente, 7500 AE Enschede, The Netherlands

Glossary:
EER: Equal Error Rate
PM-MPE: Perspective Multiplication for Multi-Perspective Enrollment
ROI: Range Of Interest
NIR: Near Infra-Red
LED: Light-Emitting Diode
PCB: Printed Circuit Board
ROC: Receiver Operating Characteristic
AUC: Area Under the Curve

I. Introduction

Biometric recognition methods are used in more applications than ever. Most modern smartphones already have one or even multiple biometric scanning sensors. One prime example is the fingerprint scanner, as nowadays over 71% of the mobile phones are equipped with a fingerprint sensor. This amount will most likely grow over the years, as these scanners become more and more standard with dropping prices. However, as these methods become more broadly used, there is an increasing risk of spoofing biometric data by abusing flaws in these designs. New biometric scanning methods are researched for increasing the security of commonly used products and systems.

One such biometric scanner is the Finger Vein Scanner. Blood vessels will become visible under Near Infrared light, and this scanner will detect the vascular pattern in the bottom part of the finger shell. In 2012, the DNB, now a part of the Data science group of the University of Twente, has done research into a different solution, which is most likely a lot harder to spoof. The idea, a finger vein scanner, is capable of capturing the vascular pattern of a finger. In recent years, more and more research has been done, improving the concept's reliability and decreasing the size of the setup.

The Finger Vein Scanner will acquire images as shown in Figure 1. The Range of Interest will then be cropped like in Figure 2. By using techniques which will be discussed in chapter II, the vascular pattern can be determined. In Figure 3, this is done by using Maximum Curvature[10]. Subsequently, an algorithm can determine genuine and impostor.

After successful testing of finger vein recognition, a new idea emerged: why limit the finger vein recognition in the 2D field? Apart from different internal and external factors, one big flaw of this method was that it was prone to deformation of the finger. Especially longitudinal rotation seemed to be a confounding factor. Therefore, a new setup was realized with 3 cameras which should in theory be able to calculate 3D images. The three images are stitched together to compute a 3D matrix of the veins. For this research we will be focusing on enabling perspective multiplication for multi-perspective, which basically captures and calculates multiple perspectives over multiple angles to compensate for a rotated finger.

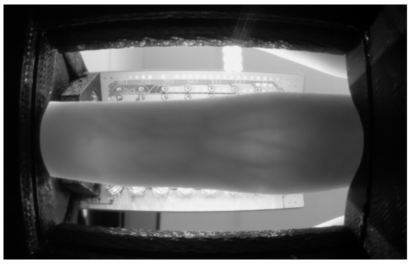

Fig. 1: Image as captured by the camera

Fig. 2: Cropped image of the finger

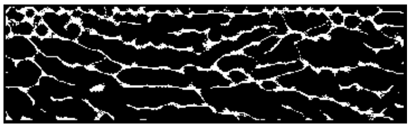

Fig. 3: Veins detected in cropped image (Maximum Curvature)

This research will create a new look into PM-MPE reconstruction of the finger's vascular pattern, and will enable 3D acquisition for future research. The setup was developed by another student of the University of Twente. Adaptations or a complete redesign could be necessary for enabling this aim, but developing a new way of vein extraction lies outside of the scope of this research.

A. Research Questions

In order to qualify the setup and its results a couple of hypotheses had to be formulated. This in turn will provide a general outline of the overall project; experiments should answer smaller sub-questions. This research focuses on two topics: Implementing the PM-MPE protocol and improving the image quality.

The following research questions were defined in advance:

1) Can the Finger Vein Scanner's image quality be improved?
   a) Is the open architecture of the casing a disadvantage?
   b) Are the cameras used adequate?
   c) Does the NIR-Filter serve a purpose?
2) Is PM-MPE imagery of the setup possible and what will be its performance?
   a) How does the EER of PM-MPE reconstruction compare to the 2D counterpart?
   b) Does PM-MPE improve on MPE with just the three cameras?
3) Can rotation of the finger be compensated?
   a) What will be the EER under different angles?
   b) Will the EER improve for rotating the finger in comparison to 2D acquisition?

II. Related Work

Lately, increasing research is taking place on the detection of finger vein patterns. This section will cover the most promising proofs of principle with regard to detection, and how they subsequently improve the quality of images.

A. *Vein detection*

Detection of veins requires some medium of detection. A useful property of the hemoglobin, a protein in the human blood, is the absorption of near-infrared light. All derivatives (i.e. altered forms) of hemoglobin show consistent results.[3][4] Especially useful is the low absorbency of bone in these NIR wavelengths[6], this way near-infrared light will be diverted through the whole finger. In the resulting near-infrared intensity graph, tissue will show up white, and veins will show up black. Detection occurs just below near surface of human fingers, as light diffracts in the finger tissue. Acquisition happens at the outside, therefore veins deeper in the finger will not be visible in images.

Hemoglobin has excellent properties for the acquisition of blood vessels. Other research was done on other acquisition techniques, for example the use of x-rays[8]. Of course this has a major downside because it involves ionizing radiation. At the present moment this method has no beneficial effects in comparison with the prevailing technique used by the detection of the hemoglobin. But it is worth noticing that there is also research into new methods.

For illumination multiple sources and locations are possible. The most common placement of the illumination is right above the finger, as for example in the Hitachi finger vein reader[7]. However, other placements are becoming more common, like the illumination from the sides or bottom. This is possible due to the aforementioned diffraction of light in the finger tissue. In most cases, the light sources which used are near-infrared LEDs, however there are other possible sources. Examples are NIR lasers (diodes), or even much simpler systems such as incandescent light bulbs, which require filtering with an NIR filter[19]. NIR LEDs are mostly chosen because of their low cost and narrow bandwidth. Another benefit of LEDs is the possibility of using Pulse Width Modulation algorithms, for illumination control.

B. *Finger vein extraction*

As earlier described, hemoglobin absorbs near-infrared light, which will in turn show as lower levels of illumination in the images (darker shades in the image). Multiple methods are already explored to subsequently extract blood vessels from the image. Therefore, devising a new method lies outside the scope of this research. Four different existing methods were researched, teach of which is described below.

A well known vessel extraction algorithm is based on repeated line tracking. To extract the patterns from the image, line-tracking operations with randomly varied starting points are repeatedly carried out. Based on the number of times the tracking lines pass through the point, a vessel will be detected.[11]

Another proposed method is using Maximum Curvature. The center lines of veins are extracted by calculating the curvature of the cross-sectional profile of the image. The paper suggests that this method is superior to conventional methods, with good robustness over varying widths and brightness levels.[10]

Song suggested a new finger vein extraction method called Mean Curvature. It uses geometrical properties of the intensity field, which makes it possible to extract the pattern from images with unclear veins.[12]

Gradient normalization and principal curvature is a method which has less restraints with regard to vein thickness and image brightness.[13].

For this research, we chose Maximum Curvature as our finger vein extraction protocol, due to its proven high quality results and easy implementation.

C. Finger deformation

Finger vein algorithms are prone to deformation of the images, as most methods rely on the finger having the same exact rotation and position in every scan.

As humans are naturally not very precise and the finger is a flexible limb, finger registration will sometimes lack accuracy with respect to the placement. This posture displacement knows six different types[9], specifically shift and rotation in all three directions. To keep these deformations as low as possible, the hardware setup should have restrictions. Small deformations can be corrected through different algorithms, however deformations of the finger can also be used for recognition purposes.

Longitudinal rotation of the finger has negative effects on the performance of the setup. In theory, acquiring enrollment images with all possible degrees of rotation would decrease these negative effects. However, this would require an infinite amount of camera angles. Multi-Perspective Enrollment (MPE), as proposed by Prommegger and Uhl[18], use multiple perspectives for acquisition during Enrollment. It states that different perspectives should be linearly spaced over different angles of the acquisition range. For authentication purposes, only one perspective is compared to all earlier acquired enrollment images using of a maximum rule score.

To further decrease the amount of camera perspectives, Perspective Multiplication was proposed[17]. Intermediary perspectives are calculated by the use of circular pattern normalization (CPN). It assumes the finger to have a circular shape, therefore supposes that the finger rolls when rotated. As shown in Figure 4, this can greatly reduce the amount of cameras required. The blue dots represent physical cameras whereas the red dots represent rotated perspectives. With the use of image processing, the enrollment image is rotated twice over a predefined angle, in this example approximately -15% and +15% degrees. Authentication will then compare the image to all three images instead of just one, thus greatly increasing performance.

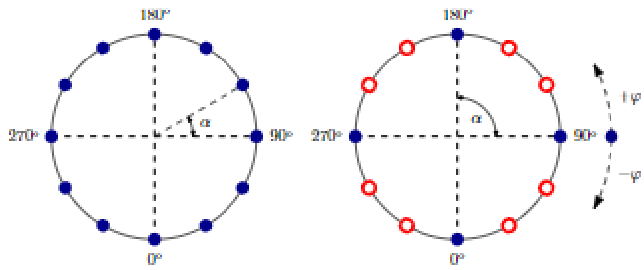

Fig. 4: Example of how PM-MPE(right) can reduce the amount of cameras as opposed to MPE(left)[17]

In plain text the protocol is defined as follows: In the Enrollment phase, η perspectives are captured, with a rotational distance of α. The two pseudo perspectives will be calculated by $\pm\phi - 1/3\alpha$ in both directions. The single perspective for authentication is captured and compared to all enrolled perspectives, which leads to $3 * \eta$ comparisons. For us this can be done for all three cameras which leads to $3 * 3 = 9$ comparisons instead of the regular 3 with MPE.

D. Image Quality

The main focus of this research was on image quality improvement by physical changes to the setup. There was not much related work on this matter, except for using a dark container to prevent ambient lighting.

However, there were some suggestions for code improvements. Firstly, Histogram equalization is proposed by multiple papers. It is a very straightforward technique to increase the global contrast of the images, and can even be undone by inversing the operation. It has one disadvantage: The calculation is indiscriminate, it may increase contrast of the the background.

A different proposed technique is Multi-Channel Gabor Filtering.[20]. This makes use of the fact that veins appear dark in the image. When rotating multiple Gabor filters(4 in this paper), and combining them, veins will appear with a lot more contrast than before.

In summary, the work presented in this paper builds on previous research to explore how others extract finger vein patterns. While earlier work focused on proposing certain acquisition methods, we focus on further improving our Finger Vein Scanner by implementing these techniques. Further, we are able to study the difference in simple 2D acquisition and perspective multiplication for multi-perspective multiplication for our scanner.

III. Methodology

For now this previously created setup was extensively tested for the use of just one camera. As earlier material already proposed, using the two secondary cameras could improve the general identification results. Enhancing the identification with multiple cameras requires images of sufficient quality. A major part of this thesis was about improving the setup and its acquisition of images. Whereafter visual reconstruction of the vessel pattern should be the next and final step.

A. Improving Setup

The first hypothesis states a crucial question about the setup's possibility of implementing PM-MPE. Earlier studies assessed 2D acquisition and identification performance. However, now all three cameras are used in conjunction with their corresponding embedded systems. The originally designed power board appeared to be underspecified, resulting in an abnormal power consumption for the power regulators. This resulted in an overvoltage on the Raspberry Pis which were destroyed in the process.

A new PCB power board was designed to prevent further damage. As displayed in Figure 5, all Raspberries and LED PCBs are now regulated by their own power regulator. Every LED draws a maximum current of 80mA. As every PCB has 8 LEDs, this results in a maximum current usage of $80*8 = 640$mA. Together with the Raspberry's current consumption of 1.2A, this stays within the power regulator's specification of 2A.

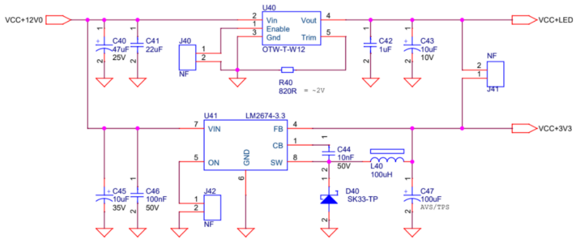

Fig. 5: Power regulation

At first the raspberries were rather provisionally attached to the sides of the setup, this made the system vulnerable to outside influences. Therefore a second advantage of the new Power board is that it acts as a Raspberry container. As seen in Figure 6 all Raspberry's are attached to the power board and reattached to the back of the system, providing a more solid base.

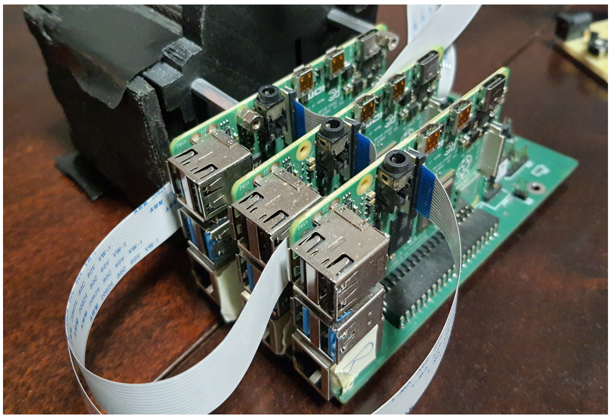

Fig. 6: Power board attached to the back of the device

In addition the new PCB has a second benefit: it acts as a communication device. Wiring of the LEDs can be attached directly to the PCB enabling I2C communication for control. At last, communication lines between both master and slave devices is established to implement interrupt based capturing of images. This will in turn drastically improve the timing in between images.

B. Improving image quality

In order to improve image quality, all factors which could have an influence should be assessed. This research focuses on physical factors instead of code implementations, and therefore lie outside the scope of this thesis.

1) NIR-Filter: The initial system had a NIR-Filter placed just beneath the finger, with the finger basically able to rest on the filter for support. At first glance this might seem like a great positioning as this would prevent finger deformation. However, grease and scratches quickly appeared, which could influence performance of acquisition. To prevent this phenomenon, adjustments were necessary. Also, the question arose if the NIR-Filter was even required.

2) LED controller: The LEDs were controlled with a PWM signal. At first, the frequency of this signal was too low (15.6 KHz). Because CMOS cameras use Rolling Shutter for acquisition, this could result in horizontal jitter. To rule out this problem, an analog controller has been chosen. As shown in Figure 7, each LED can be individually adjusted by means of a potentiometer, so problems with PWM frequencies are excluded.

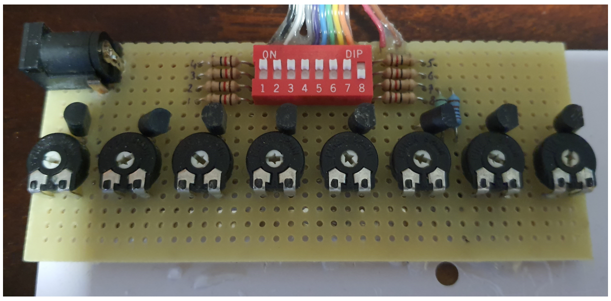

Fig. 7: Analog LED controller

3) LED Side illumination: Although a drop angle of just 3°is specified for the LEDs, they are still visible on the two outer cameras. This results in less visibility of the finger region and an overall higher grey value. As shown in Figure 8, the outer cameras are exposed to stray light. Therefore, a modification was made which created some form of cover.

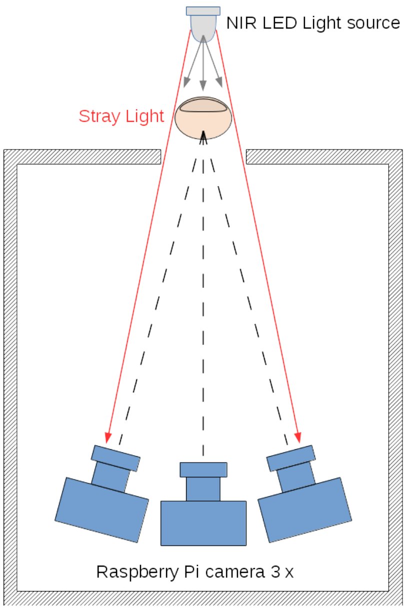

Fig. 8: Stray light of LEDs

4) Ambient lighting: Effects of ambient lighting and background noise had to assessed. Due to its open structure, the system is very prone to objects and light sources from above. These can either be objects which reflect and/or produce NIR light, which will in turn result in artifacts. This can act as a problem for edge detection of the finger, effecting the ROI.

C. Perspective Multiplication for Multi-Perspective Enrollment

PM-MPE calculates pseudo-perspectives in between the existing camera perspectives. To get a clear grasp on this protocol, an example image is presented in Figure 9. The images represents a cross section of the finger in the middle with two pseudo-perspectives either side. Blood vessels are shown as blue dots, with the projected vessels on the surface of the finger in red.

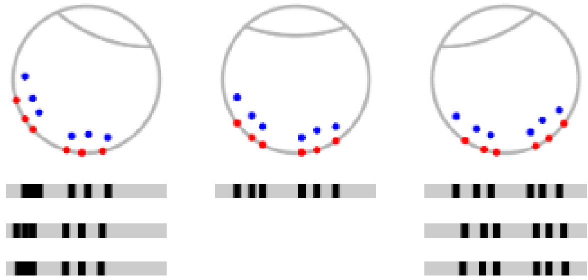

Fig. 9: Principle of pseudo-perspectives[17]

The bars underneath the cross-sections show a visual representation of the blood vessels. When rotating the finger, projection of the vessels will also shift. The middle cross-section only has 1 bar as both the projected as the actual vessel are perpendicular to the bar. When the finger is rotated, the projected vessel will rotate a little further than the actual vessel. In order to compensate for this phenomenon, a shifting of the image is performed. This is done on the initial image, not on the extraction.

For the calculation of the pseudo-perspectives, the position of a pixel within the ROI extracted from the Enrollment image is defined by its x-coordinate x_{enrol} and the corresponding y-coordinate y_{enrol}, which is calculated by III-C

$$y_{enrol} = \sqrt{r^2 - x_{enrol}^2} \tag{1}$$

where r is the approximated radius of the finger. r is half the finger width, which corresponds to half of the height of the extracted finger ROI. The rotation for the pseudo perspective is calculated by applying the rotation matrix given in III-C

$$\begin{bmatrix} x_{pseudo} \\ y_{pseudo} \end{bmatrix} = \begin{bmatrix} cos(-\theta) & -sin(-\theta) \\ sin(-\theta) & cos(-\theta) \end{bmatrix} * \begin{bmatrix} x_{enrol} \\ y_{enrol} \end{bmatrix} \quad (2)$$

x_{pseudo} and y_{pseudo} are the coordinates of the vein pixel in the pseudo-perspective and θ is the rotation angle. The actual image for the pseudo perspective is calculated from the grey values at x_{pseudo} using linear interpolation.

After calculating the remapping, cubic interpolation was used to perform various geometrical transformations of the 2D images. Image content is not affected but the pixel grid is deformed to the destination image. To prevent sampling artifacts the mapping is done in reverse order, from destination to source.

$$dst(x, y) = src(fx(x, y), fy(x, y)) \quad (3)$$

This is done pixel-wise for each pixel of the destination image. It will then use its corresponding donor pixel to compute new values with the function above. Extrapolation of non-existing pixels are filtered as these have no effect on the newly formed image. Interpolation however will be done by bicubic interpolation, as multiple pixels from the original image could be remapped to the same pixel.

IV. Results and Analysis

A. Dataset

A new dataset was acquired using a custom routine with the University of Twente Finger Vein Scanner. Due to the Covid-19 crisis, finger images of only a few test subjects could be acquired.[2] However, the intention of this research was not to identify and thus verify its real EER, but to compensate for rotation of the finger. It contains images of 1 subject, capturing both hands, 6 finger images per subject, with every finger rotated under 17 different angles. Therefore, 6 different image sets are present. Every image subset is defined as follows:

Field	**Description**	**Value**
date	Day of acquisition	yyyymmdd
subject_ID	ID of subject which took place	S0...S99
session_ID	ID of the session	0..9
finger_ID	ID of the finger left little=1 .. right little = 8	0-8
Rotation	Theta of capture	-30% .. 30%

Thus resulting in a form of: <date>_<finger_ID>_<session_ID>_<Rotation>

B. Experiments

As the title of the article already suggests, this project was more about enabling PM-MPE than about implementing it. The main contribution of this work will be improving performance of the setup. The upcoming experiments should answer or supplement the hypotheses stated in chapter III.

1) Placement of NIR-Filter: At first the NIR-Filter was placed beneath the finger region. Now we would like to know if this placement is optimal or other placements are possible as well. Therefore three different locations were proposed:

1) Beneath the finger
2) In the middle of the setup
3) Behind the camera lens

All three different propositions have their own pros and cons, these will now be summarized. The results were verified by visual inspection, as calculating a score would be redundant

Beneath the finger (current situation): This is very prone to grease and scratches from the finger. However, replacing the filter would be the easiest and cheapest because of the smaller region it spans. Because the filter is so far up, not a lot of distortion is visible from angular refraction. One severe deficit of the implementation is the deformation of the finger itself. The finger lays on top of the filter, thus deforming from its circular form to a more oval form, which in turn decreases the effectiveness of the PM-MPE protocol.

In the middle of the setup: This an alternative to the current situation. Although it avoids the finger deformation problem, it has its own image deformation problem. As the filter has a thickness, angular refraction will occur. Although it protects the sensitive camera equipment, it is also prone to accumulating dust, which could result in artefacts. In the end, this will be the least compelling alternative.

Behind the camera lens: We chose for positioning the filter behind the lens, as this had the least amount of drawbacks. The NIR-Filter is protected from dust and scratches, and no deformation will occur.

However, a small modification was necessary for this implementation: the filter had to be cut in a circular sizeby a water-jet and which would then be glued to back of the lens.

2) Spectrum Analysis: Experiments take place in a laboratory of the University of Twente, which is lit by eco-friendly LEDs. These LEDs are visible on imagery, resulting in artefacts. Therefore, a spectrum analysis is performed to identify the intervening wavelengths in order to block these. For this experiment, a spectrum analyser of Avantes brand was used. First, the NIR blocking potential of the filter will be analysed. As shown in Figure 10, outdoor lighting has a very broad spectrum which is excellent for this experiment. While still facing outdoor lighting, the NIR-Filter is

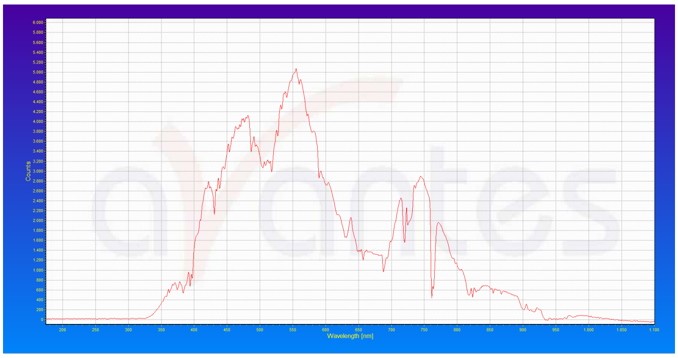

Fig. 10: Spectrum of outdoor lighting

placed in front of the sensor. As shown in Figure 12, all wavelengths below 760nm are fully blocked by this high pass filter. CMOS sensors are able to detect wavelengths up to 1000nm. This ensures that all NIR wavelengths are well within the camera's received spectrum.

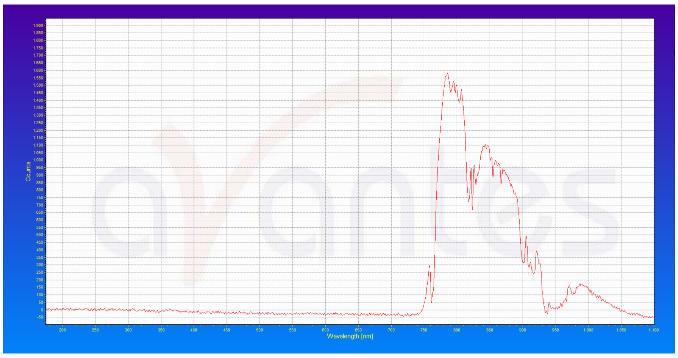

Fig. 11: Spectrum of outdoor lighting through NIR-Filter

3) Closed or Open Architecture: Most finger vein scanners have a closed architecture. Our scanner is unique in the fact that it is open from above, but unfortunately this comes with challenges. Problems can arise because the camera is now open to external influences. An open architecture was chosen because it ensures that the system is a lot more accessible for test subjects. People are less hesitant to lay their finger into an open construction than to insert it into the dark opening of an unknown device. For now there are several possibilities to extract the ROI without including the background, we decided to keep an open architecture. For the future, a different topology is suggested but it requires a complete redesign.

4) LED side illumination: Although a beam angle of just 3°is specified for the LEDs, they are still visible from the outer cameras as shown in Figure 8. This results in less visibility of the finger region and an overall higher grey value. Therefore, an adjustment was made: a cover was mounted on the LED PCB preventing illumination from the sides to be reflected into both outer cameras.

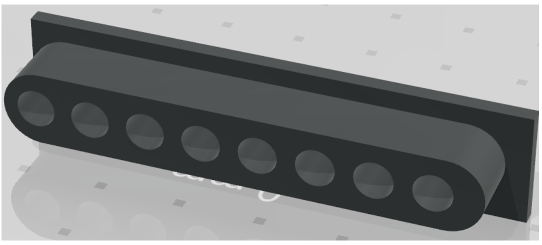

Fig. 12: Cover which is mounted over LED PCB

Although stray light is counteracted on in most cases, sometimes when the finger is not positioned correctly on the LED cover, unwanted light will still appear. This has major negative effects on image quality, resulting in stray light being acquired on images, as shown in Figure 13. In the recommendations an alternative for this problem is suggested.

Fig. 13: Stray light still appears on outer camera

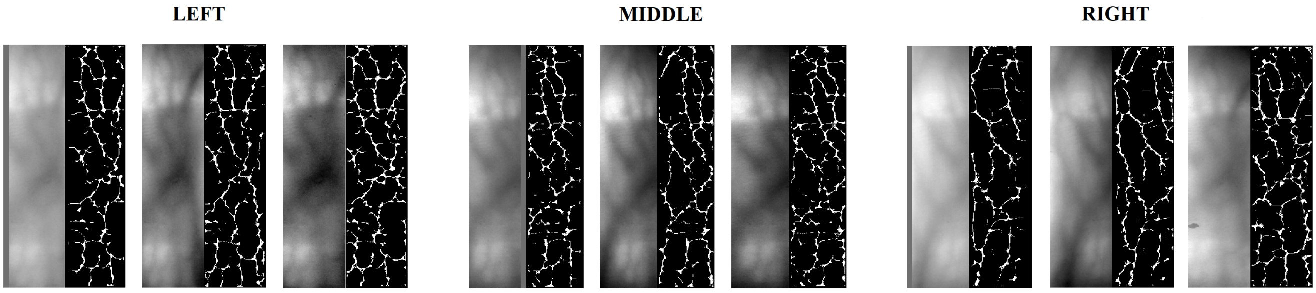

Fig. 14: Images of all three cameras with their respective pseudo perspectives ($\pm\phi = 10°$)

C. Recognition Tool Chain

Multiple steps are required for obtaining the finger vein pattern, the implementation of which is explained in the following steps:

1) *Finger Region Detection:* A mask of the finger is created by the well known lee region protocol.
2) *ROI Extraction:* After a mask is obtained, a rectangle with the width and position of the finger is multiplied with the original image.
3) *Perspective Multiplication:* Before feature extraction, other perspectives are created.
4) *Feature Extraction:* The Maximum Curvature method is used.
5) *Comparison:* A score is calculated, e.g. Miura match

D. Perspective multiplication

The PM-PME protocol was implemented successfully. As shown in Figure 15, the original image(left) was rotated for $\phi = 10°$ resulting in a pseudo-perspective (right). The pseudo-perspective is a rotated version from the original; parts which contain no information due to interpolation are filled with the average grey value.

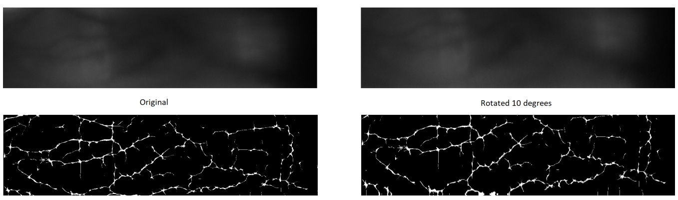

Fig. 15: Perspective Multiplication

Multiple rotational distances were proposed with α = -10°and 10°. For one of the data sets an example is shown in Figure 14.

Results are verified by a series of comparisons. Checking images, images which we like to compare to their genuine data set, are matched against enrollment images. The finger is rotated between -40 and +40 degrees to see effects of rotation on the score. For this test we use the Miura match protocol which has a score from 0 to 0.5, where 0.5 is a perfect match. The images have a resolution of 960x540 pixels, and scores will most likely be higher when images of lower resolution are used. Due to time constraints an actual comparison between image resolution and scores was not included. All the tests are enumerated below:

1) **1 cam:** Images of only the middle camera will be matched
2) **1 cam - 3 cam:** Checking images of the middle camera will be matched with all 3 enrollment images
3) **Full 3 cam:** All 3 checking images are matched with all 3 enrollment images
4) **1 cam - PM-MPE:** Checking image of the middle camera is matched with all 3 enrollment images and their pseudo-perspectives
5) **3 cam - PM-MPE:** All 3 checking images are matched with all 3 enrollment images and their pseudo-perspectives
6) **Full PM-MPE:** All 3 checking images with their pseudo-perspectives are matched with all 3 enrollment images and their pseudo-perspectives

As shown in Figure 16, Full PM-PME shows better score results across all rotations. Promegger et al compared 1 camera to PM-MPE enrollment images, therefore this research had a whole new depth in this topic. All different possible PM-MPE protocols are listed and compared against each other. As expected the 1 camera protocol falls off at around 10°. The image quality of the outer cameras is probably on the

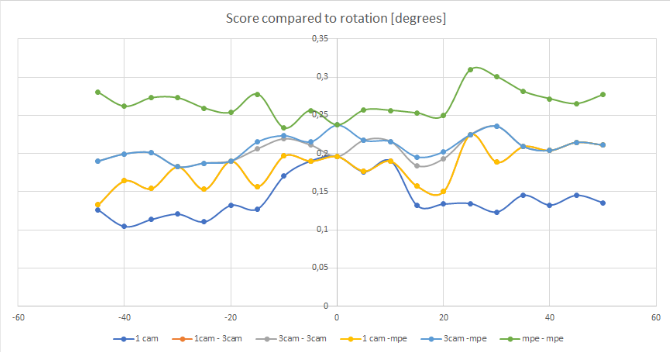

Fig. 16: Performance results (Scores) for every rotation

low end as the 3 camera solution has troubles with achieving a higher score at the ±30° point. Comparing the 3 individual images to PM-MPE has a way higher score at the outer degrees, this is probably because of the pseudo-perspectives. Scoring of Full PM-PME is the highest, but is it therefore better? The simple answer is no: images of both the left and the right camera have a different brightness because of the way light is travelling through the finger. As shown in Figure 17, outer camera images are a lot brighter. In future research these effects should be cancelled by either changing shutter speed or image processing.

Nevertheless, Full PM-MPE appears to work better on cameras with with different qualities. This is of course a positive effect, especially for circumstances where cameras of a lesser quality are used. For now, computing Full PM-MPE takes too much time for authentication purposes. However, most of the code is written in Matlab and computation time can thus drastically be improved by switching to to e.g. Python.

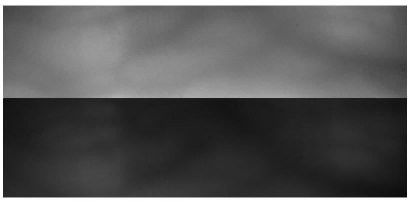

Fig. 17: Difference in acquisition images of Right (top) and Middle (bottom) cameras

As shown Figure 18, a data set of an imposter has a drastically lower score than a genuine data set. Therefore, a threshold of around 0.19 can be set. A full comparison of all the acquired data sets is displayed in Appendix VI-.4. Here, all scores are compared as in Figure 16; for some fingers, full PM-MPE has a less compelling effect compared to standard PM-MPE. For some data sets the method shows abnormalities in the form of the 1 camera method having more spread. This is most likely due to human error as rotating the finger inside of the device is hard.

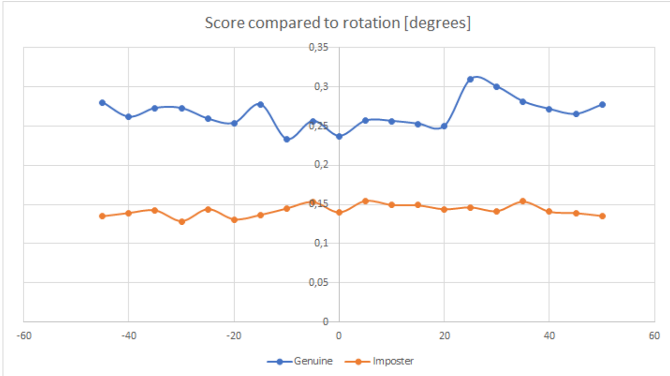

Fig. 18: Different scores for genuine and imposter set

Although the full data set consists of only of 6 different fingers three score matrices are shown in Figure 19. Here we can examine if Full PM-MPE has the ability to distinguish between imposter and genuine fingers. These graphs are purely for indication, as the data set is way too small for certainty. When we no examine the newly acquired Score matrix we will see that our earlier defined threshold of 0.19 appears to hold. However, in some cases the difference between the score and the threshold seems to be small, lowering the threshold will reduce false negative scores. For now, results seem promising as there are no mismatches. The whole score matrix has a standard deviation of 0.0358; genuine scores have standard deviation of 0.0242 and imposter of 0.0306. Lowering the resolution of the images in a future research will probably increase the standard deviation of the whole set, resulting in fewer mismatches. In the end, further research should include a far larger data set.

	1	2	3	4	5	6
K_L_M	0,2132	0,1645	0,1271	0,1384	0,1353	0,1281
K_L_R	0,1671	0,2492	0,1628	0,1501	0,1648	0,1568
K_L_W	0,1445	0,1626	0,238	0,1467	0,1476	0,139
K_R_M	0,1429	0,157	0,138	0,23	0,1401	0,1511
K_R_R	0,1341	0,1665	0,1486	0,1554	0,2069	0,1434
K_R_W	0,1472	0,1605	0,1334	0,1389	0,1413	0,2728

Fig. 19: Score matrix

V. Conclusion

This article proved that implementation of the PM-MPE by Promegger et al. was applicable. In addition new method is introduced: Full PM-MPE. Instead of just comparing the image of the middle camera, all the cameras are used with their corresponding pseudo-perspectives. This drastically improved performance on the more extreme rotations of the finger. For authentication purposes the code should be rewritten as the Matlab code is too slow for real life use cases. Aside from protocol implementation it adjusted and suggested multiple improvements to the current setup for image quality improvement.

We will now answer the earlier defined research questions:
Can the Finger Vein Scanner's image quality be improved? Major steps have been made in improving image quality. At first, it was impossible to even capture images with multiple cameras. A new PCB was designed to overcome electrical issues and enabling interrupt based capturing. Side illumination was drastically reduced by mounting a cover on the LEDs. NIR Filter placement was adjusted, this prevented dust and scratched on the filter. Nevertheless, there are still some adjustments to be made: side illumination should be counteracted on; objects directly above the setup still influence the lee region results and implementing Black and White cameras should increase overall quality

Is PM-MPE imagery of the setup possible and what will be its performance? The PM-MPE protocol of Promegger et al. is implemented succesfully, in addition a new method is formed: Full PM-MPE. This method also uses the outer cameras as well as the pseudo-perspectives for authentication purposes. The performance of this setup is unknown: a larger data set has to be acquired in further research.

Can rotation of the finger be compensated? Yes, results show that a rotations of $\pm 40^{\circ}$ still appear to be validated by authentication. For larger rotations problems will arise, the setup would then require more cameras. This will happen because veins will on the side of the finger are less visible than those on the bottom.

All in all, PM-MPE and Full PM-MPE are fully implemented and results look promising. More research still has to be done in context of image quality. Thereafter, a larger data set has to be acquired to fully compute an EER for this device.

VI. Recommendations

In hindsight, as also concluded in Chapter V, images captured by the cameras in the existing setup have a somewhat lower quality than expected. Therefore multiple recommendations are made in this chapter.

1) Black and white camera: Because only grayscale images are needed, processing power is wasted as the camera's CMOS sensor is a an RGB type, and all three colour channels are averaged. Therefore the use of black and white cameras, which the ”old setup” actually did use, is recommended for further research. RGB pixels have a filter which could block NIR wavelengths, increasing noise. In the end, black/white pixels have a higher area size, which decreases the amount of illumination required.

2) Closed encasing: Due to the setup's open design, which was chosen for its invitational nature, a lot of background noise could decrease performance. Ambient lighting could have a huge impact on performance, depending on the positioning of said device. Placing it beneath an artificial light source increases artefacts at the edges of the finger and decreases visibility of the vascular pattern within the finger region. Lastly, when using the lee region protocol, all objects on the ceiling can influence the range of interest.

3) Improved illumination control: As the paper already mentioned, the earlier designed light algorithm did not produce consistent results. In this research, a manually adjusted setup was made to increase stability. However, this resulted in an enormous decrease of acquisition speed when different fingers were provided. This negates the whole idea of an automated acquisition device. Therefore, a more consistent lighting protocol should be devised.

4) Improved LED cover: Stray light is a massive problem in the current situation. Therefore, a different kind of LED cover is recommended; for example a concept could be some form of rubber cradle attached to the existing cover. The finger should then be pushed against its surface, which should decrease stray light to a bare minimum. This is however against the nature of an open architecture, but will reduce artefacts for authentication purposes. A disadvantage about this concept is the hassle of keeping the cradle hygienic.

ACKNOWLEDGMENT

I would like to thank my supervisors Raymond Veldhuis and Luuk Spreeuwers for their guidance and general advice. Furthermore I want to thank my friends and family for helping my motivation.

REFERENCES

[1] Rikkerink, K.B.W. Research Topics: Enabling Perspective Multiplication for Multi-Perspective Finger Vein Scanner .

[2] Rivm.nl. 2020. De Ziekte COVID-19 — RIVM. [online] Available at: ¡https://www.rivm.nl/coronavirus-covid-19/ziekte¿ [Accessed 5 June 2020].

[3] HORECKER, Bernard L. The absorption spectra of hemoglobin and its derivatives in the visible and near infra-red regions. J. biol. Chem, 1943, 148.1: 173-183.

[4] irk J. Faber, Egbert G. Mik, Maurice C. G. Aalders, and Ton G. van Leeuwen, "Light absorption of (oxy-)hemoglobin assessed by spectroscopic optical coherence tomography," Opt. Lett. 28, 1436-1438 (2003)

[5] EMERSON, W. H.; FISCHER, E. E. The infra-red absorption spectra of carbonate in calcified tissues. Archives of Oral Biology, 1962, 7.6: 671-683.

[6] COTÉ, Charles J., et al. The Effect of Nail Polish on Pulse Oximetry. Anesthesia & Analgesia, 1988, 67.7: 683-686.

[7] HITACHI LTD., Finger Vein Authentication : White Paper. 2006

[8] TOSHIBA, N. Niki ; Y. Kawata ; H. Satoh ; T. Kumazaki 3D imaging of blood vessels using X-ray rotational angiographic system. 1993

[9] Huang, B.N., Liu, S.L., Li, W.X.: A finger posture change correction method for finger-vein recognition. In: Proceedings of Symposium on Computational Intelligence for Security and Defence Applications, Ottawa, Canada, pp. 1–7 (2012)

[10] Miura N., Nagasaka A., Miyatake T.; Extraction of Figer-Vein Patterns Using Maximum Curvature Points in Image Profiles. Conference on Machine Vision Applications. 2005

[11] Miura N., Nagasaka A., Miyatake T.; Feature extraction of finger-vein patterns based on repeated line tracking and its application to personal identification. Conference on Machine Vision Applications. 2004

[12] SONG, Wonseok, et al. A finger-vein verification system using mean curvature. Pattern Recognition Letters, 2011, 32.11: 1541-1547.

[13] CHOI, Joon Hwan, et al. Finger vein extraction using gradient normalization and principal curvature. In: Image Processing: Machine Vision Applications II. International Society for Optics and Photonics, 2009. p. 725111.

[14] HARTLEY, Richard I.; STURM, Peter. Triangulation. Computer vision and image understanding, 1997, 68.2: 146-157.

[15] ELKOURA, George; SINGH, Karan. Handrix: animating the human hand. In: Proceedings of the 2003 ACM SIGGRAPH/Eurographics symposium on Computer animation. Eurographics Association, 2003. p. 110-119.

[16] RUSU, Radu Bogdan; COUSINS, Steve. 3d is here: Point cloud library (pcl). In: 2011 IEEE international conference on robotics and automation. IEEE, 2011. p. 1-4.

[17] B. Prommegger and A. Uhl, "Perspective Multiplication for Multi-Perspective Enrollment in Finger Vein Recognition," 2019 International Conference of the Biometrics Special Interest Group (BIOSIG), Darmstadt, Germany, 2019, pp. 1-6.

[18] Prommegger, Bernhard; Uhl, Andreas: Rotation Invariant FingerVein Recognition. In: Proceedings of the IEEE 10th International Conference on Biometrics: Theory, Applications, and Systems(BTAS2019). Tampa, Florida, USA, 2019.

[19] The return of the incandescent lamp? [online] Available at: ¡https://www.ee.co.za/article/return-incandescent-lamp.html¿ [Accessed 4 April 2021]

[20] J. Yang and J. Yang, "Multi-Channel Gabor Filter Design for Finger-Vein Image Enhancement," 2009 Fifth International Conference on Image and Graphics, Xi'an, China, 2009, pp. 87-91,

[21] M. Abdullah-Al-Wadud, M. H. Kabir, M. A. Akber Dewan and O. Chae, "A Dynamic Histogram Equalization for Image Contrast Enhancement," in IEEE Transactions on Consumer Electronics, vol. 53, no. 2, pp. 593-600, May 2007

APPENDIX

This appendix includes all data comparisons with regards to rotation. There is a lot of fluctuation in the performance of the algorithm. This is most likely due to human error, except for the index finger rotating for exactly 5°is hard. For now the algorithm seems promising, future studies should include more data.

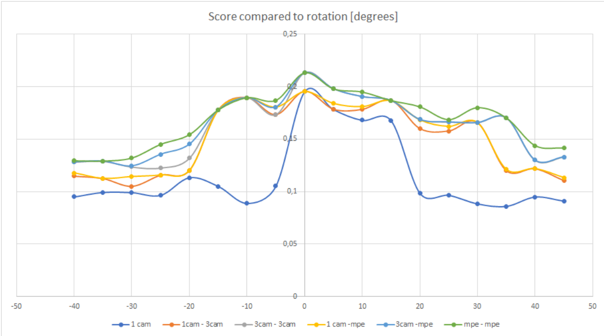

Data set 1 : Left middle finger

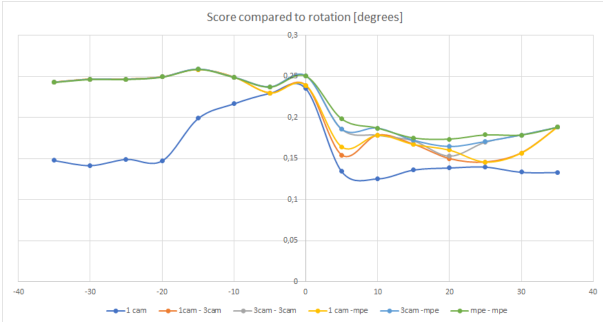

Data set 2 : Left ring finger

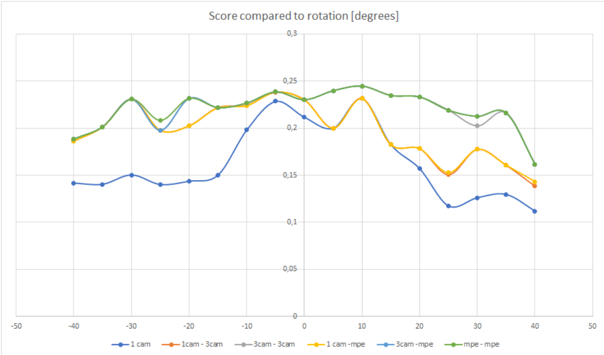

Data set 3 : Left index finger

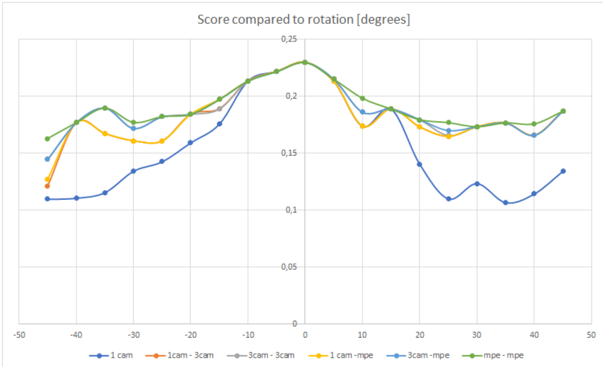

Data set 4 : Right middle finger

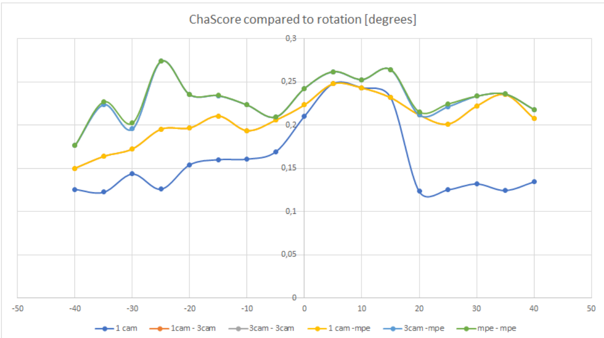

Data set 5 : Right ring finger

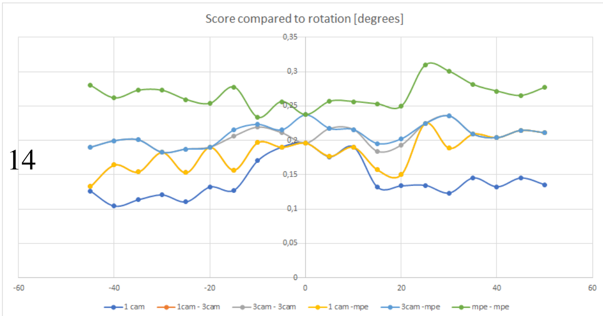

Data set 6 : Right index finger